Cell Reports

Pro-resolving lipid mediator lipoxin A_4 attenuates neuro-inflammation by modulating T cell responses and modifies the spinal cord lipidome

Graphical abstract

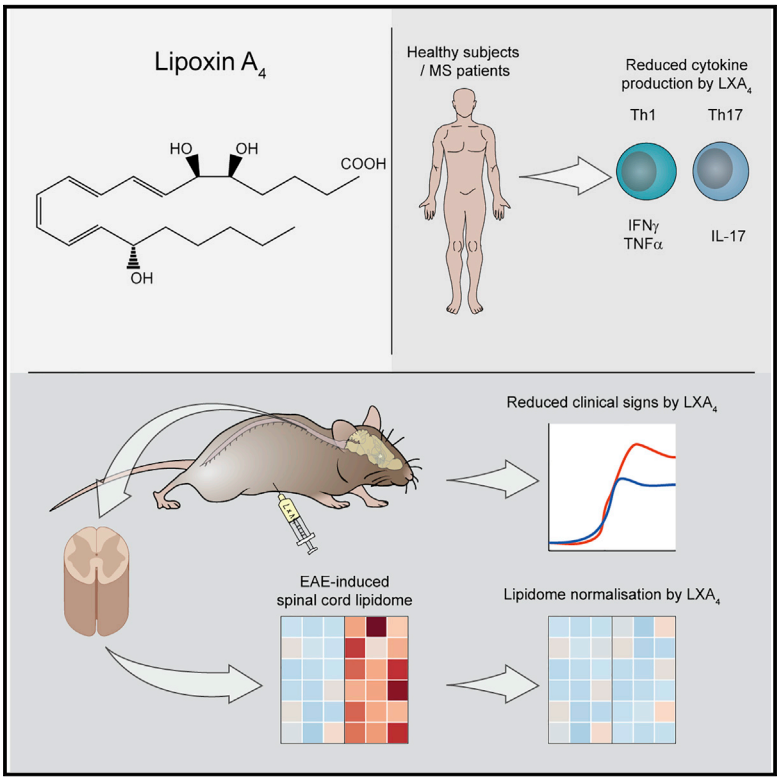

Highlights

- LXA_4 ameliorates clinical signs of EAE by dampening Th1 and Th17 effector functions
- LXA_4 modulates Th1 and Th17 responses from healthy controls and patients with MS
- Characterization of the spinal cord lipidome under healthy and EAE conditions
- LXA_4 normalizes the EAE-induced spinal cord lipidome

Authors

Claudio Derada Troletti, Gaby Enzmann, Valerio Chiurchiù, ..., Helga E. de Vries, Britta Engelhardt, Gijs Kooij

Correspondence

g.kooij@amsterdamumc.nl

In brief

Derada Troletti et al. demonstrate that boosting a protective resolution response by lipoxin A_4 (LXA_4) suppresses clinical signs in a neuro-inflammatory animal model for multiple sclerosis (MS). They provide critical mechanistic insights into LXA_4-mediated amelioration of neuro-inflammation and thereby highlight the potential clinical application of LXA_4 for MS.

Derada Troletti et al., 2021, Cell Reports *35*, 109201
June 1, 2021
https://doi.org/10.1016/j.celrep.2021.109201

CellPress

Cell Reports

CellPress
OPEN ACCESS

Report

Pro-resolving lipid mediator lipoxin A_4 attenuates neuro-inflammation by modulating T cell responses and modifies the spinal cord lipidome

Claudio Derada Troletti,[1,2,7] Gaby Enzmann,[2,7] Valerio Chiurchiù,[3,4,7] Alwin Kamermans,[1] Silvia Martina Tietz,[2] Paul C. Norris,[6] Neda Haghayegh Jahromi,[2] Alessandro Leuti,[5] Susanne M.A. van der Pol,[1] Marijn Schouten,[1] Charles N. Serhan,[6] Helga E. de Vries,[1,8] Britta Engelhardt,[2,8] and Gijs Kooij[1,6,8,9,*]

[1]MS Center Amsterdam, Department of Molecular Cell Biology and Immunology, Amsterdam Neuroscience, Vrije Universiteit Amsterdam, Amsterdam UMC, De Boelelaan 1117, 1081 Amsterdam, the Netherlands
[2]Theodor Kocher Institute, University of Bern, 3012 Bern, Switzerland
[3]Institute of Translational Pharmacology, National Research Council, 00133 Rome, Italy
[4]Laboratory of Resolution of Neuroinflammation, European Center for Brain Research, IRCCS Santa Lucia Foundation, 00179 Rome, Italy
[5]Department of Medicine, Campus Bio-Medico University of Rome, Via Alvaro del Portillo 21, 00128 Rome, Italy
[6]Center for Experimental Therapeutics and Reperfusion Injury, Department of Anesthesiology, Perioperative and Pain Medicine, Brigham and Women's Hospital, Harvard Medical School, Boston, MA 02115, USA
[7]These authors contributed equally
[8]Senior author
[9]Lead contact
*Correspondence: g.kooij@amsterdamumc.nl
https://doi.org/10.1016/j.celrep.2021.109201

SUMMARY

The chronic neuro-inflammatory character of multiple sclerosis (MS) suggests that the natural process to resolve inflammation is impaired. This protective process is orchestrated by specialized pro-resolving lipid mediators (SPMs), but to date, the role of SPMs in MS remains largely unknown. Here, we provide *in vivo* evidence that treatment with the SPM lipoxin A_4 (LXA_4) ameliorates clinical symptoms of experimental autoimmune encephalomyelitis (EAE) and inhibits $CD4^+$ and $CD8^+$ T cell infiltration into the central nervous system (CNS). Moreover, we show that LXA_4 potently reduces encephalitogenic Th1 and Th17 effector functions, both *in vivo* and in isolated human T cells from healthy donors and patients with relapsing-remitting MS. Finally, we demonstrate that LXA_4 affects the spinal cord lipidome by significantly reducing the levels of pro-inflammatory lipid mediators during EAE. Collectively, our findings provide mechanistic insight into LXA_4-mediated amelioration of neuro-inflammation and highlight the potential clinical application of LXA_4 for MS.

INTRODUCTION

Multiple sclerosis (MS) is the most common chronic inflammatory disorder of the central nervous system (CNS), characterized by blood-brain barrier disruption, immune cell infiltration into the CNS, demyelination, and neurodegeneration (Reich et al., 2018). Although it is still debated whether inflammation and/or autoimmunity are at the root of the disease (Stys et al., 2012), there is extensive evidence for a crucial role of the immune system in disease pathogenesis (Lassmann, 2005; Sawcer et al., 2011). Particularly, genome-wide association studies have identified over 230 genetic loci commonly associated with MS, the majority of which are linked to genes associated with the immune system, T cell activation, and proliferation, thereby implicating the peripherally activated $CD4^+$ T cells in MS pathogenesis (Cotsapas and Mitrovic, 2018; Hellberg et al., 2016; Sawcer et al., 2011). Moreover, the abundant presence of inflammatory cells in CNS lesions of patients with MS or in its experimental model experimental autoimmune encephalomyelitis (EAE), has led to the hypothesis that MS is mediated by pathogenic T cell responses against myelin antigens, followed by neurodegeneration (Compston and Coles, 2008). As a result, the majority of the current therapies consist of immunosuppressive or anti-inflammatory agents, which are effective in early stages of the disease but often result in severe side effects and eventually fail to prevent disease progression (Chiurchiù, 2014). Therefore, there is an urgent need to develop alternative approaches allowing not only to interfere with chronic neuro-inflammation but also to promote local tissue recovery and subsequent homeostasis.

The chronic neuro-inflammatory character of MS suggests that the natural process to resolve inflammation (resolution of inflammation) is not properly functioning (Newson et al., 2014; Serhan, 2014). Resolution of inflammation is an active process mediated by specialized pro-resolving lipid mediators (SPMs), which are synthetized from ω-3 or ω-6 polyunsaturated fatty acids. Among these, E and D series resolvins, protectins, and maresins are

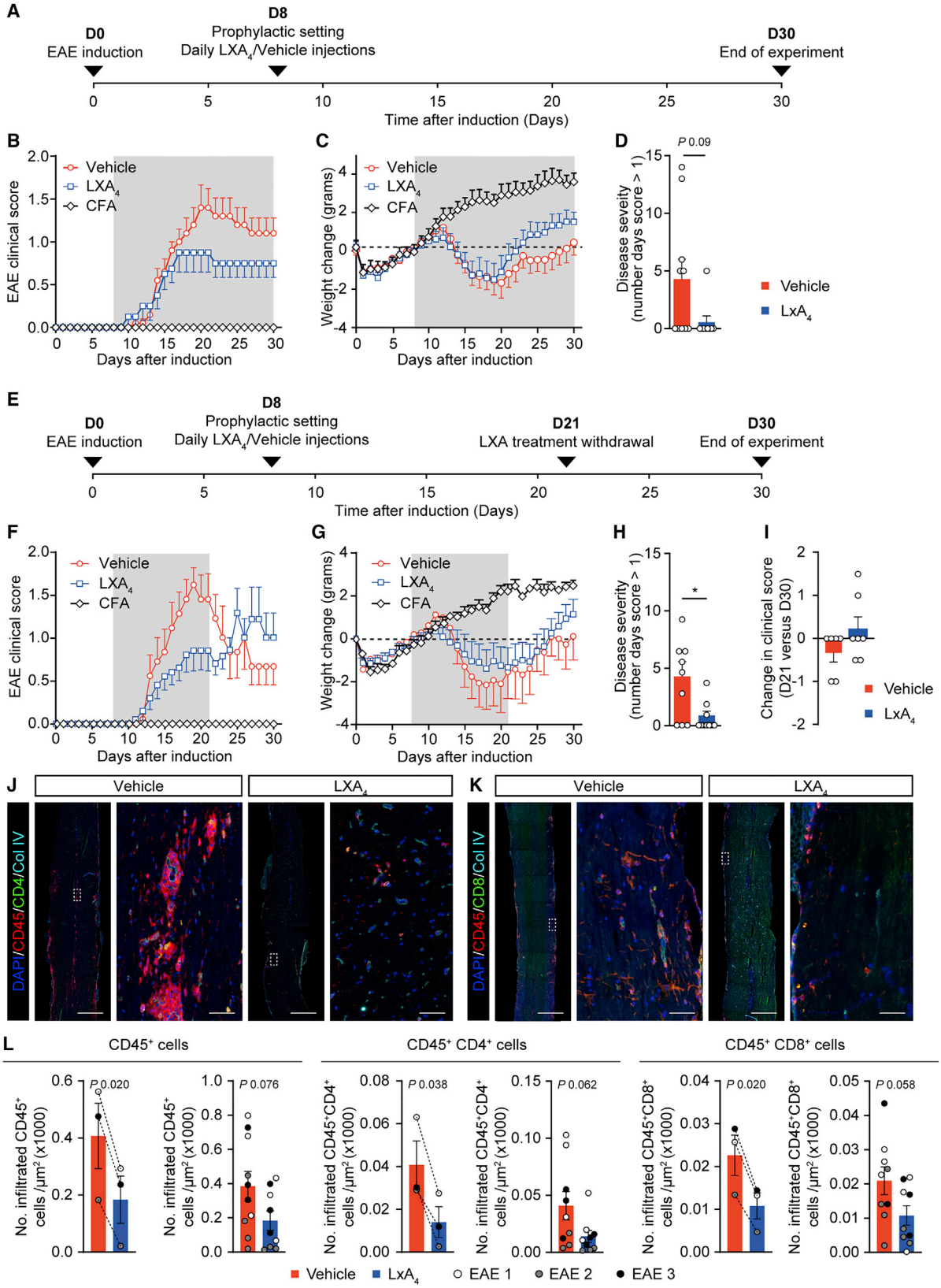

(legend on next page)

derived from ω-3 polyunsaturated fatty acids eicosapentaenoic acid (EPA) and docosahexaenoic acid (DHA), respectively. SPMs of the lipoxin family include lipoxin A_4 (LXA_4) and LXB_4 as well as their isomeric isoforms aspirin-triggered lipoxin (Serhan, 2005), which are biosynthesized from arachidonic acid (AA) (Calder, 2006; Serhan, 2014; Serhan and Petasis, 2011). In general, SPMs actively promote resolution of inflammation via specific mechanisms that include limiting neutrophil recruitment, enhancing efferocytosis, and pathogen removal, as well as reducing the secretion and production of pro-inflammatory mediators (Gilroy et al., 2004; Serhan, 2014) and reactive oxygen species (Leuti et al., 2019), thereby promoting the cardinal signs of resolution. Despite the beneficial effects in various chronic inflammatory disease models (Chiurchiù et al., 2018), the potential role of the resolution program and SPMs in MS and neuro-inflammation in general remains to be investigated.

Importantly, we recently showed that LXA_4 levels were not increased in plasma of patients with relapsing-remitting MS compared to healthy controls (Kooij et al., 2020), providing first evidence for a potential resolution defect in MS. These findings are in line with earlier observations in the cerebrospinal fluid of patients with highly active MS compared to those with inactive disease (Prüss et al., 2013). Due to the robust neuro-inflammatory character of MS in combination with the potent anti-inflammatory and pro-resolving capacities of LXA_4, we hypothesized that this SPM may represent an innovative strategy to limit neuro-inflammation in the context of MS. We here show that daily injections of LXA_4 ameliorate EAE clinical symptoms, reduce CNS infiltration of $CD4^+$ and $CD8^+$ T cells, dampen Th1 and Th17 effector T cell functions, and potently modulate the inflammatory responses of encephalitogenic T lymphocytes from patients with relapsing-remitting MS. Moreover, we provide evidence that the spinal cord lipidome is severely altered during EAE and that LXA_4 administration normalizes these effects by specifically dampening pro-inflammatory lipid mediators derived from AA. Overall, these findings highlight the therapeutic potential of LXA_4 in MS and provide detailed insight into its mechanism of action in counteracting neuro-inflammation.

RESULTS

LXA_4 treatment ameliorates EAE clinical signs

To study the effect of LXA_4 treatment on neuro-inflammation *in vivo*, we induced EAE in female C57BL/6J mice and subjected them to a prophylactic treatment regimen. Mice received daily intraperitoneal injection of 100 ng LXA_4/mouse or ethanol (1% in saline) as a vehicle control, starting prior to onset of the disease (day 8) until the end (Figure 1A). Interestingly, LXA_4 treatment ameliorated EAE clinical scores and counteracted the reduction in the body weight compared to EAE vehicle-treated mice (Figures 1B and 1C). In particular, we observed a strong trend toward reduction in the severity of the disease between the LXA_4-prophylactic-treated mice and the vehicle-treated mice (Figure 1D; Tables S1 and S2). To provide more insights into the mode of action of LXA_4 and to understand in which time window it exerts its protective actions, we investigated the effect of LXA_4 withdrawal on clinical signs of EAE. To achieve this, LXA_4 was injected from day eight but withdrawn after day 21, leaving the animals untreated for the remainder of the experiment (until day 30; Figure 1E). Importantly, LXA_4 treatment significantly reduced clinical signs of EAE (Figure 1F), the mean clinical score at the peak of the disease, and disease severity compared to the vehicle-treated EAE mice (Figure 1H; Tables S1 and S3), with a slight impact on weight changes of the animals (Figure 1G). Interestingly, LXA_4 cessation at day 21 elicited a rebound effect, resulting in a worsening of EAE symptoms when compared to the last day of the treatment period. In contrast, the vehicle-EAE group displayed a reduction in EAE scores (Figure 1I; Table S3). Overall, these findings suggest that LXA_4 ameliorates EAE and that its presence is required to continuously dampen neuro-inflammation and suppress clinical symptoms of EAE.

LXA_4 inhibits $CD4^+$ and $CD8^+$ T cell migration into the CNS during EAE

Because the main neuro-inflammatory hallmark in MS pathology is represented by an abundant infiltration of peripheral

Figure 1. LXA_4 treatment ameliorates clinical signs of EAE

(A) Timeline illustrating the experimental setup of the treatment regimen of EAE mice.

(B) Clinical EAE scores of vehicle-treated mice (1% ethanol; n = 10 mice), LXA_4-treated mice (n = 8 mice; 100 ng/animal/day) and CFA/control mice (n = 9) until 30 days after EAE induction (treatment period highlighted in gray).

(C) Change in body weight, expressed in grams compared to day 0.

(D) Disease severity at day 30 p.i. of vehicle or LXA_4-treated mice.

(B–D) Results are presented as mean ± SEM.

(E) Timeline illustrating the experimental setup of the "LXA_4-withdrawal" EAE experiment.

(F) Clinical EAE scores of vehicle-treated mice (n = 9), LXA_4-treated mice (treatment period: day 8 until day 21 p.i.; n = 10), and CFA/control mice (n = 10) until 30 days after EAE induction (treatment period highlighted in gray).

(G) Change in body weight, expressed in grams compared to day 0.

(H) Disease severity at day 21 p.i. of vehicle or LXA_4-treated mice. Results are presented as mean ± SEM. *$p < 0.05$ determined by Mann Whitney test.

(I) Rebound effect: change in EAE clinical scores of vehicle-treated mice (n = 6 mice) and LXA_4-treated mice (n = 7 mice) after LXA_4 treatment cessation (day 21 versus day 30 after EAE induction), presented as mean ± SEM.

(J and K) Representative pictures of $CD45^+$ (red), $CD4^+$ (J), $CD8^+$ (K) cells (green), collagen IV (cyan; vasculature), and DAPI (blue; nuclei) immunohistochemical stainings of cervical spinal cord sections from EAE-vehicle-treated and LXA_4-treated mice (day 8–30 p.i.) sacrificed at the peak of the disease (day 21 p.i.; n = 7–9 biological replicates/group). Scale bars, overview: 1 mm and inset: 50 μm.

(L) Quantification of $CD45^+$, $CD4^+$, and $CD8^+$ infiltrated cells in the spinal cord parenchyma of LXA_4- and vehicle-treated EAE mice. Left graph displays average number of infiltrated cells per EAE (n = 3 EAE experiments, 3 mice/group/EAE; dotted line connects values of individual EAE experiments); right graph displays the average number of infiltrated cells of individual mice (n = 7–9 biological replicates/group); data points are color-coded according to the individual EAE experiment. Results are presented as mean ± SEM. *$p < 0.05$ determined by paired (left graph) or unpaired (right graph) Student's t test.

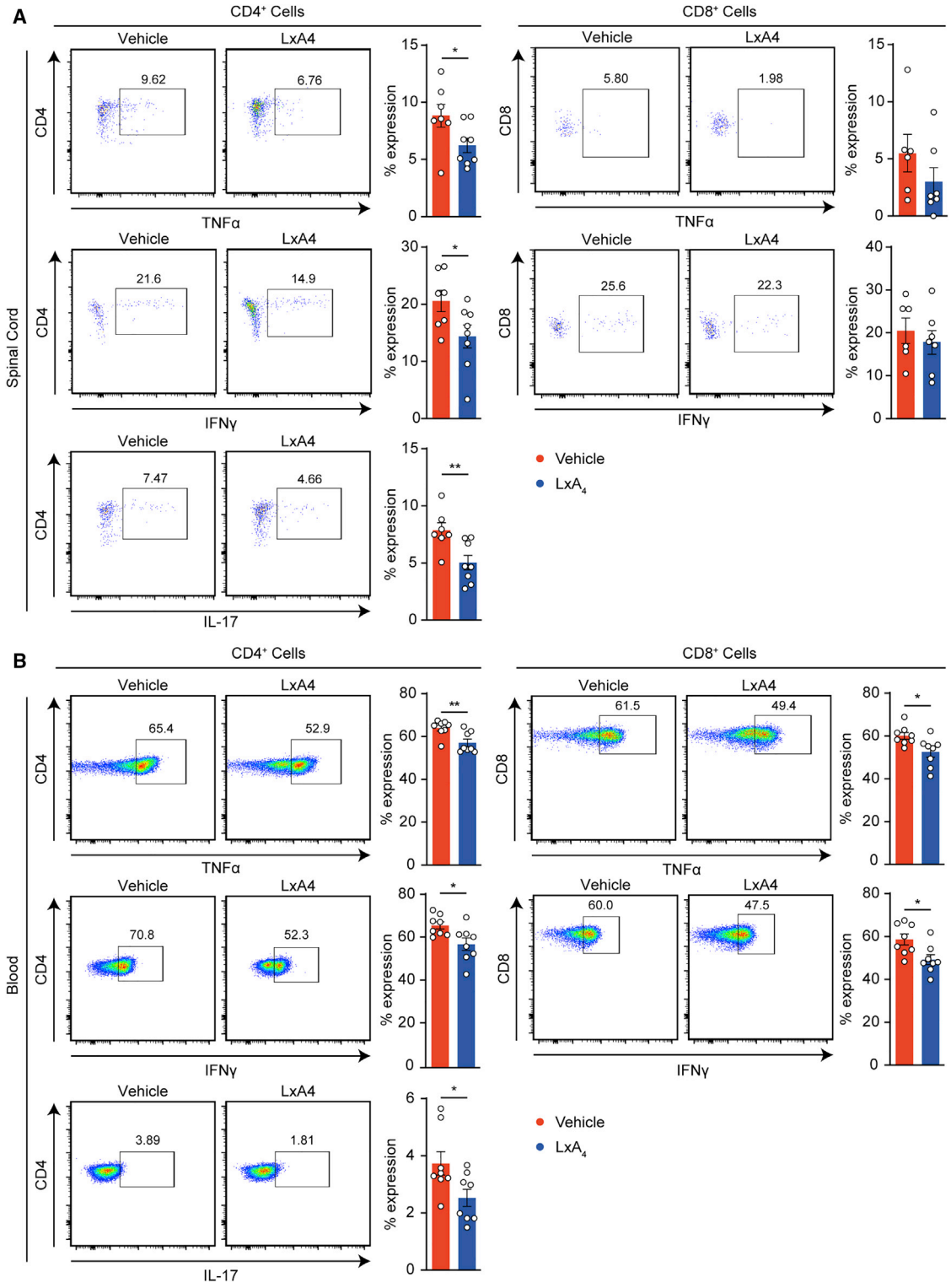

Figure 2. LXA_4 reduces central and peripheral cytokine responses

Immune cell populations were isolated from LXA_4- or vehicle-treated EAE mice at peak of disease and analyzed by flow cytometry, as described in the STAR Methods.

(A) Representative flow cytometry plots and bar graphs from spinal cord infiltrates showing percentages of intracellular production of TNF-α, IFN-γ, and IL-17 from $CD4^+$ T cells (left panel) or TNF-α and IFN-γ from $CD8^+$ T cells (right panel). Results are presented as mean ± SEM of 6–8 individual mice/group. *$p < 0.05$ and **$p < 0.01$, as determined by Student's t test.

(legend continued on next page)

leukocytes into the CNS, and particularly in the spinal cord, we next sought to determine whether LXA_4 was able to modulate leukocyte recruitment in EAE mice. Accordingly, we isolated the spinal cord of LXA_4-treated versus vehicle-treated mice and performed immunohistochemical analysis to quantitatively assess the extent of leukocyte infiltration into the CNS parenchyma at the peak of the disease (Figures 1J and 1K). Interestingly, upon LXA_4 treatment, we observed a significant reduction of infiltrating $CD45^+$ leukocytes in the spinal cord parenchyma compared to vehicle-treated EAE mice at the peak of disease in three independent experiments (Figures 1J–1L). As the $CD45^+$ population contains both pro- and anti-inflammatory cells, we next focused on the main pathogenic cells that mediate myelin damage during MS, which are autoreactive $CD4^+$ and $CD8^+$ T lymphocytes, especially interferon (IFN)-γ-producing Th1 and interleukin-17 (IL-17)-producing Th17 subsets, whose presence is abundant in cerebrospinal fluid and MS lesions (Compston and Coles, 2008; Han et al., 2014; Lassmann, 2014). Importantly, further characterization of the $CD45^+$ spinal cord infiltrates revealed that both $CD4^+$ and $CD8^+$ T cell subsets were significantly decreased upon LXA_4 treatment compared to vehicle-treated EAE animals (Figures 1J–1L). Overall, these *in vivo* findings suggest that LXA_4 treatment ameliorates EAE clinical symptoms and attenuates neuro-inflammation by affecting $CD4^+$ and $CD8^+$ T cell infiltration into the CNS.

LXA_4 modulates central and peripheral mouse Th1 and Th17 responses

To further address the underlying mechanism of action, we next assessed whether LXA_4 was able to impact effector T cell responses in terms of cytokine production. For this, we examined lymphocytes from both the spinal cord and blood of EAE mice upon LXA_4 treatment compared to vehicle-treated EAE mice at the peak of disease. We specifically evaluated encephalitogenic Th1 and Th17 responses in terms of tumor necrosis factor alpha (TNF-α), IFN-γ (for both $CD4^+$ and $CD8^+$ T cells), and IL-17 (for $CD4^+$ T cells; see Figure S1 for gating strategies). Importantly, in the spinal cord, LXA_4 significantly reduced the percentage of infiltrated $CD4^+$ T cells producing TNF-α, IFN-γ, and IL-17, whereas a similar trend was observed for $CD8^+$ T cells (Figure 2A). Moreover, upon anti-CD3 and anti-CD28 stimulation of peripheral lymphocytes isolated from LXA_4-treated versus vehicle-treated EAE mice, we observed a significant reduction in both $CD4^+$ and $CD8^+$ T cell responses in terms of TNF-α, IFN-γ, and IL-17 cytokine production (Figure 2B). Overall, these data suggest that the LXA_4-induced amelioration of EAE course and severity might be due to a reduction of Th1 and Th17 effector functions, both centrally and peripherally.

LXA_4 modulates human Th1 and Th17 responses

To translate these findings to a human setting, we next addressed whether LXA_4 was able to also impact human T cell responses and whether it was able to affect their transendothelial migration capacity. For this, we investigated human T cells from patients with relapsing-remitting MS as well as healthy controls (Table S4). In particular, the immunomodulatory role of LXA_4 was investigated upon polyclonal activation of the T cell receptor with anti-CD3 and anti-CD28 (Figure 3A). We found that activated T cells showed a significantly induced expression of CD25, which was not affected by LXA_4 in both control and relapsing-remitting MS patient-derived T cells (Figure 3B). To further assess the effect of LXA_4 on specific T cell subsets, we also investigated cytotoxic $CD8^+$ T cells and $CD4^+$ Th1 and Th17 cells. As expected and previously shown (Gentile et al., 2020), anti-CD3 and anti-CD28 stimulation resulted in high percentages of TNF-α-, IFN-γ-, and IL-17-producing T cells in both controls and patients with relapsing-remitting MS (Figures 3D–3G). Of note, cytokine production from all T cell subsets was higher in patients with relapsing-remitting MS, accounting for the hyper-activation of these pathogenic cells in MS. Importantly, LXA_4 treatment significantly reduced the percentage of TNF-α-producing $CD8^+$ T cells of healthy subjects (Figure 3C) and IFN-γ-producing $CD8^+$ T cells of both healthy subjects and patients with relapsing-remitting MS (Figure 3D). Moreover, LXA_4 significantly reduced the percentage of IL-17- and TNF-α-producing $CD4^+$ T cells of healthy subjects, but not from patients with relapsing-remitting MS (Figures 3E and 3F), although the percentage of IFN-γ-producing cells was reduced by LXA_4 both in healthy and relapsing-remitting-MS-patient-derived $CD4^+$ T cells (Figure 3G). In view of these results, we next sought to investigate the effect of LXA_4 on the transendothelial migration capacity of $CD4^+$ and $CD8^+$ T cells by using a human *in vitro* blood-brain barrier model (Kooij et al., 2010, 2014). As shown in Figures 3H and 3I, treatment with LXA_4, significantly inhibited the migration of both human T cell subsets across inflamed brain endothelial cells. Overall, these results indicated that the production of specific cytokines that characterize the main pro-inflammatory T cell subsets from control or patients with MS was significantly reduced or showed a trend toward significance upon pre-treatment with LXA_4, indicating that LXA_4 regulates human T cell responses as well as their transmigration capacity.

Lipid mediator alterations in the spinal cord during EAE

Besides extensive infiltration of various leukocyte subsets into the CNS, EAE is also characterized by local microglia and astrocyte activation, which together results in clinical signs (Engelhardt and Ransohoff, 2005). To further characterize this pro-inflammatory CNS milieu during EAE and address the question whether CNS inflammation is reflected by changes in lipid mediator profiles, we performed targeted lipid mediator metabololipidomics using liquid chromatography-tandem mass spectrometry (LC-MS/MS) by analyzing 42 distinct lipid mediators based on published criteria (i.e., matching chromatographic retention times [RTs], fragmentation patterns, and six characteristic and diagnostic ions; Colas et al., 2014). For this, we analyzed spinal cords from control and EAE mice during the peak and chronic phase of the disease. Accordingly, we identified lipid mediators from each of the ω-6 AA, ω-3 DHA, and EPA bioactive

(B) Representative flow cytometry plots and bar graphs of matching peripheral blood samples showing percentages of intracellular production of TNF-α, IFN-γ, and IL-17 from $CD4^+$ T cells (left panel) or TNF-α and IFN-γ from $CD8^+$ T cells (right panel) upon re-stimulation with anti-CD3/CD28. Results are presented as mean ± SEM of 6–8 individual mice/group. *$p < 0.05$ and **$p < 0.01$, as determined by Student's t test.

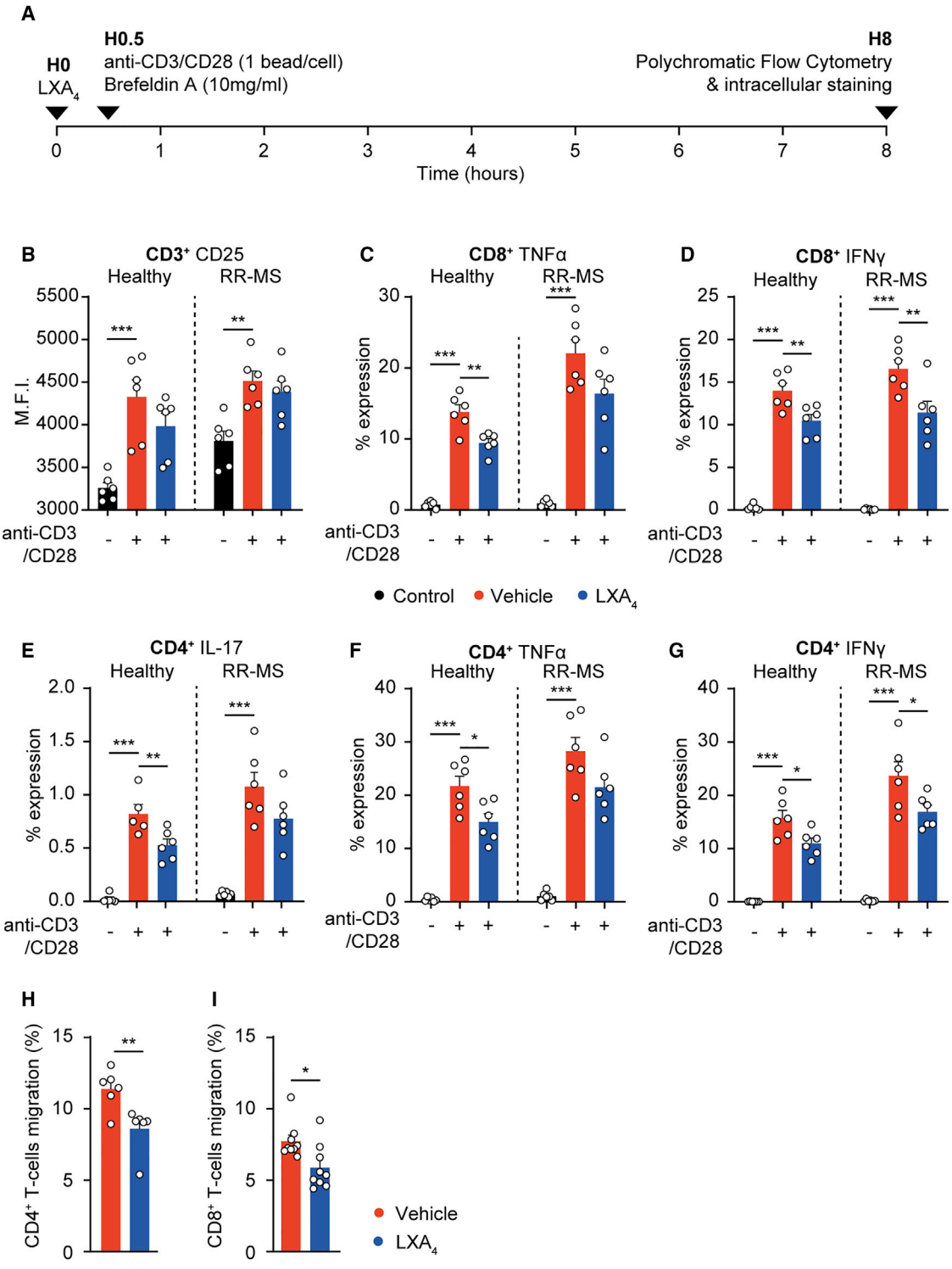

Figure 3. LXA_4 reduces cytokine responses in activated human T cell populations from control and patients with relapsing-remitting (RR)-MS

(A) Schematic representation of the experimental procedure: peripheral blood mononuclear cells (1×10^6 cells per well) were left untreated (black bars) or treated with vehicle (red bars) or LXA_4 (10 nM; blue bars) for 30 min. Cells were then stimulated with anti-CD3/CD28 for 8 h, stained at the cell surface and intracellularly, and analyzed by flow cytometry.

(B) Mean fluorescence intensity (MFI) of CD25 surface expression in total $CD3^+$ T cells.

(C and D) Percentages of intracellular production of (C)TNF-α and (D) IFN-γ from $CD8^+$ T cells.

(legend continued on next page)

metabolomes (Table 1; complete lipid mediator stereochemistry and annotated biological functions have been previously described; Dalli and Serhan, 2012). We identified several SPMs in the spinal cord of control and EAE mice, including LXA_4, LXB_4, resolvin D2 (RvD2), resolvin D3 (RvD3), maresin-1 (Mar1), resolvin E2 (RvE2), aspirin-triggered PD1 (AT-PD1), and resolvin E3 (RvE3) as well as various key pathway markers (Table 1; Figure S2). Importantly, we observed that neuro-inflammation predominantly affected the AA bioactive metabolome by revealing significantly increased expression levels of pro-inflammatory prostaglandins like prostaglandin E_2 (PGE_2), prostaglandin D_2 (PGD_2), prostaglandin F_{2a} (PGF_{2a}), leukotriene B_4 (LTB_4), and thromboxane (TXB_2) during the chronic phase of disease as well as the peak of disease (PGE_2) compared to (Complete Freund's Adjuvant, CFA) control mice (Table 1; Figures 4A–4D and S2). We also observed significantly increased levels of various AA and EPA pathway markers, like 5-HETE, 15-HETE, 5-HEPE, and 18-HEPE, during different stages of EAE compared to CFA (Table 1). Together, these findings provide a detailed characterization of lipid mediator profiles in the spinal cord of control and EAE mice.

Reduced pro-inflammatory lipid mediators upon LXA_4 treatment during EAE

We next addressed the question whether the LXA_4-mediated amelioration of clinical signs could be explained by local and beneficial changes in the spinal cord lipidome during the peak and chronic phase of EAE. Importantly, LXA_4 treatment significantly increased LXA_4 expression levels in the spinal cord during different stages of EAE (Table 1), thereby revealing LXA_4-CNS incorporation upon treatment. As shown in Figures 4A–4D, we observed that LXA_4 treatment predominantly suppressed the AA bioactive metabolome by revealing significantly reduced levels of pro-inflammatory prostaglandins, like PGE_2, at both the peak and during the chronic phase of EAE, whereas PGD_2, PGF_{2a}, LTB_4, and TXB_2 were significantly reduced during the chronic phase of EAE upon LXA_4 treatment (Figures 4A–4D; Table 1). In contrast, a key AA pathway marker (15-HETE) was significantly reduced upon LXA_4 treatment during the chronic phase of EAE, whereas 5-HETE was significantly reduced upon LXA_4 treatment at the peak of EAE, similar to DHA and EPA pathway markers, like 7-HDHA and 5-HEPE, respectively (Table 1). Of note, besides LXA_4, none of the identified SPMs in the spinal cord were significantly affected by LXA_4 treatment (Figure 4D; Table 1). Such targeted metabololipidomic fingerprinting was also confirmed by using unbiased principal-component analysis (PCA), showing that each experimental group was associated to a distinct lipid mediator profile and that LXA_4 treatment resulted in a normalized lipid mediator signature that closely resembles the control group (Figure 4E). Taken together, these findings indicate that LXA_4 treatment either directly and/or indirectly (via the regulation of T cell responses) affects the expression levels of pro-inflammatory lipid mediators during EAE, thereby suppressing ongoing neuro-inflammation in the spinal cord.

DISCUSSION

This study provides critical evidence that boosting a protective resolution response by LXA_4 treatment suppresses clinical signs of EAE *in vivo* and reduces neuro-inflammation, therefore illustrating the therapeutic potential of LXA_4. Particularly, we observed a significant reduction in disease severity upon LXA_4 treatment as well as a reduction of $CD4^+$ and $CD8^+$ T cell infiltration into the CNS during EAE. Moreover, LXA_4 treatment suppressed the pro-inflammatory T cell responses both centrally and peripherally during EAE but also in healthy and MS-derived T cells and blocked their migratory capacity, thereby substantiating the immunomodulatory properties of LXA_4 in a human setting. Finally, we provided evidence for substantial lipid mediator alterations in the spinal cord during EAE and show that LXA_4 administration normalizes these effects by specifically dampening pro-inflammatory lipid mediators, like prostanoids. Overall, our findings indicate that LXA_4 may represent a promising approach to curtail neuro-inflammation and can be potentially considered as a therapeutic tool to limit MS disease progression.

Dysfunction of endogenous resolution programs may contribute to chronic inflammation, a pathological feature of several diseases (Serhan, 2014; Tabas and Glass, 2013). The evidence for both anti-inflammatory and pro-resolving properties of several SPMs, including LXs, indicates that SPMs are powerful pro-resolving lipid mediators that can profoundly affect several aspects associated with neurological disorders, like Alzheimer's disease (Medeiros et al., 2013; Wang et al., 2015), Parkinson's disease (Krashia et al., 2019), focal cerebral ischemia (Hawkins et al., 2014; Wu et al., 2010, 2013; Ye et al., 2010), spinal cord injury (Martini et al., 2016), traumatic brain injury (Bisicchia et al., 2018; Luo et al., 2013; Ren et al., 2017), and also EAE (Poisson et al., 2015). Particularly, AT-LXA_4 treatment reduced nuclear factor κB (NF-κB) activation and levels of pro-inflammatory mediators, as well as increased levels of anti-inflammatory cytokines, ultimately promoting alternative-activated microglia and reducing AD-like pathology in mice (Medeiros et al., 2013). Moreover, it has been shown that the levels of LXA_4 in the cerebrospinal fluid and in the hippocampus of patients with Alzheimer's disease were lower compared to the level of control subjects and that this decrease was correlated with the degree of cognitive deficit and tissue accumulation of tau protein (Wang et al., 2015). Nevertheless, the potential impact of LXs and other SPMs in pathological aspects of specific CNS

(E–G) Percentages of intracellular production of (E) IL-17, (F) TNF-α, and (G) IFN-γ from $CD4^+$ T cells.
(B–G) Results are presented as mean ± SEM of six biological replicates. $^{**}p < 0.01$ and $^{***}p < 0.001$, as determined by one-way ANOVA followed by post hoc Bonferroni correction. Confluent brain endothelial cells (BECs) were stimulated for 24 h with TNF. Human $CD4^+$ T or $CD8^+$ T cells (1×10^5 cells/well) were treated with LXA_4 (10 nM) or vehicle (ethanol) for 30 min prior to being plated on BECs. Cells were incubated in a co-culture setting for 4 h before harvesting the transmigrated cells.
(H and I) Percentage of (H) $CD4^+$ or (I) $CD8^+$ T cell transmigration evaluated by flow cytometry. Data are presented as mean ± SEM of 3 biological replicates done in triplicate. $^{**}p < 0.01$ compared to control (vehicle-treated T cells) determined by Student's t test.

Table 1. Mouse EAE spinal cord lipid mediator (LM)-SPM signature profile upon LXA_4 treatment

AA bioactive metabolome	Q1	Q3	CFA	EAE peak + vehicle	EAE peak + LXA_4	EAE end + vehicle	EAE end + LXA_4
AA	303	259	5,606.1 ± 353.2	5,532.0 ± 543.7	5,285.2 ± 457.0	5,225.0 ± 866.2	4,386.1 ± 161.6
LTB_4	335	195	1.98 ± 0.30	1.11 ± 0.04	1.11 ± 0.07	5.58 ± 1.72[a]	1.02 ± 0.25[b]
20-OH-LTB_4	351	195	–	–	–	–	–
20-COOH-LTB_4	365	195	–	–	–	–	–
5*S*,12*S*-diHETE	335	195	0.36 ± 0.08	0.29 ± 0.02	0.24 ± 0.07	0.71 ± 0.34	0.23 ± 0.09
5*S*,15*S*-diHETE	335	115	–	–	–	–	–
PGD_2	351	189	542.0 ± 99.3	857.2 ± 74.6	694.1 ± 27.3	1,564.9 ± 162.5[c]	558.3 ± 139.4[b]
PGE_2	351	189	337.8 ± 89.6	1,445.0 ± 156.6[c]	651.4 ± 122.5[d]	1,564.2 ± 148.8[c]	871.4 ± 99.3[e]
PGF_{2a}	353	193	95.21 ± 8.68	136.47 ± 4.73	138.39 ± 23.81	392.64 ± 79.56[c]	179.54 ± 7.70[b]
TXB_2	369	169	175.1 ± 85.4	309.3 ± 43.5	314.76 ± 93.5	926.8 ± 104.4[c]	246.4 ± 48.0[e]
15-HETE	319	219	231.1 ± 43.3	273.1 ± 39.3	298.3 ± 71.6	846.7 ± 107.9[c]	309.4 ± 34.7[e]
12-HETE	319	179	167.18 ± 54.14	477.53 ± 193.36	181.13 ± 28.68	74.44 ± 6.58	89.10 ± 15.57
5-HETE	319	115	30.80 ± 2.65	86.99 ± 24.07[a]	29.15 ± 3.28[d]	19.75 ± 2.26	22.47 ± 2.81
LXA_4	351	115	0.33 ± 0.02	0.34 ± 0.03	0.56 ± 0.05[f]	0.25 ± 0.03	0.49 ± 0.05[g]
LXB_4	351	115	1.30 ± 0.17	2.13 ± 0.43	1.80 ± 0.24	2.10 ± 0.64	0.72 ± 0.18[g]
AT-LXA_4	351	115	0.18 ± 0.04	0.22 ± 0.07	0.24 ± 0.04	0.40 ± 0.09	0.14 ± 0.12
AT-LXB_4	351	221	–	–	–	–	–
DHA bioactive metabolome							
DHA	327	283	13,765 ± 958	14,624 ± 884	14,365 ± 690	12,542 ± 1,699	10,931 ± 556
RvD1	375	215	–	–	–	–	–
RvD2	375	215	0.25 ± 0.04	0.26 ± 0.10	0.27 ± 0.13	0.17 ± 0.05	0.29 ± 0.11
RvD3	375	181	0.11 ± 0.03	0.13 ± 0.03	0.12 ± 0.02	0.15 ± 0.04	0.19 ± 0.04
RvD4	375	255	–	–	–	–	–
RvD5	359	199	–	–	–	–	–
RvD6	359	101	–	–	–	–	–
PD1	359	153	–	–	–	–	–
AT-PD1	359	153	0.32 ± 0.13	0.31 ± 0.04	0.18 ± 0.06	0.20 ± 0.05	0.19 ± 0.06
PDX	359	153	0.75 ± 0.27	0.22 ± 0.05	0.44 ± 0.14	1.25 ± 0.38	0.56 ± 0.16
Maresin 1	359	221	0.19 ± 0.02	0.54 ± 0.18	0.53 ± 0.27	0.65 ± 0.32	0.47 ± 0.06
7*S*,14*S*-diHDHA	359	221	0.41 ± 0.09	0.76 ± 0.12	0.42 ± 0.12	0.51 ± 0.19	0.59 ± 0.18
17-HDHA	343	245	13.61 ± 4.05	6.11 ± 1.22	7.83 ± 1.53	23.18 ± 8.10	9.48 ± 1.01
14-HDHA	343	205	36.82 ± 19.48	57.72 ± 25.88	18.50 ± 1.62	7.99 ± 0.68	10.06 ± 2.67
7-HDHA	343	141	4.47 ± 0.86	8.11 ± 1.56	4.53 ± 0.26[f]	3.07 ± 0.27	3.09 ± 0.35
4-HDHA	343	101	10.77 ± 1.39	13.32 ± 0.83	11.00 ± 2.20	8.69 ± 0.49	8.42 ± 2.05
EPA bioactive metabolome							
EPA	301	257	1,693.4 ± 220.4	1,771.6 ± 279.5	2,114.1 ± 793.8	1,723.0 ± 214.1	1,440.7 ± 112.2
RvE1	349	195	–	–	–	–	–
RvE2	333	253	1.57 ± 0.33	1.57 ± 0.27	0.78 ± 0.19	0.74 ± 0.15	0.64 ± 0.13
RvE3	333	201	6.31 ± 0.38	8.66 ± 0.84	6.76 ± 1.51	6.04 ± 1.42	4.83 ± 0.33
18-HEPE	317	259	11.40 ± 1.38	10.67 ± 1.28	16.74 ± 5.55	27.45 ± 7.27[a]	15.27 ± 0.63
15-HEPE	317	219	29.90 ± 18.17	27.93 ± 12.33	12.67 ± 0.28	18.63 ± 2.83	14.63 ± 4.48
12-HEPE	317	179	20.77 ± 4.11	54.24 ± 20.14	25.46 ± 6.02	11.78 ± 0.99	14.36 ± 5.19
5-HEPE	317	115	4.22 ± 0.33	7.92 ± 1.26[h]	4.96 ± 0.72[f]	3.87 ± 0.32	4.13 ± 1.04

AA, DHA, and EPA bioactive metabolome signature profile (pg/100 mg tissue) determined from the spinal cord of vehicle-treated mice, LXA_4-treated mice (day 8–30 p.i.), and CFA control mice at the peak of the disease (day 21 p.i.) and at the end of the disease (day 30 p.i.; CFA: n = 5 mice; all other groups: n = 3 mice). Data are presented as means (pg/100 mg spinal cord) ± SEM, and statistical significance is determined by one-way ANOVA followed by post-hoc Bonferroni correction

[a]$p < 0.05$ compared to CFA

[b]$p < 0.01$ compared to EAE end + vehicle

[c]p < 0.001 compared to CFA
[d]p < 0.01 compared to EAE peak + vehicle
[e]p < 0.001 compared to EAE end + vehicle
[f]p < 0.05 compared to EAE peak + vehicle
[g]p < 0.05 compared to EAE end + vehicle
[h]p < 0.01 compared to CFA

disorders, such as MS, is still largely unknown (Bogie et al., 2020). To date, only one study has shown an impaired resolution program in the cerebrospinal fluid of patients with MS (Prüss et al., 2013). However, the aforementioned study has several limitations, mainly due to the limited amount of patient material and the lack of appropriate control groups. Nevertheless, the authors showed that, in particular, LXA_4 levels were not increased in patients with highly active MS. Importantly, these findings are in line with our recent observations in plasma of patients with relapsing-remitting MS compared to healthy controls (Kooij et al., 2020), which together prompted us to elucidate the role of LXA_4 during neuro-inflammation in more detail in the present manuscript.

Here, we show direct beneficial effects of LXA_4 treatment on neuro-inflammation during EAE via reducing clinical signs, limiting $CD4^+$ and $CD8^+$ T cell infiltration into the CNS and dampening central and peripheral Th1 and Th17 effector functions. LXA_4 withdrawal during the chronic phase of EAE resulted in a rebound effect, which suggests that presence of LXA_4 is required to continuously dampen neuro-inflammation and prevent resurgence of clinical signs of the disease. Our results confirm and extend previous observations where DHA (Kong et al., 2011) and RvD1 (Poisson et al., 2015) ameliorate neuro-inflammation and reduce clinical signs of EAE, as well as recent studies showing LXA_4-mediated inhibition of microglial activation and reduction of neuro-inflammation in spinal cord injury (Martini et al., 2016) and ischemic stroke (Hawkins et al., 2017). In a mouse EAE study, RvD1 induced a profound reduction in the number of $CD4^+$ T cells infiltrating the CNS (Poisson et al., 2015). In light of these findings and to address the abundance of T cells in the cerebrospinal fluid of patients with MS (Han et al., 2014) as well as in MS lesions (Lassmann, 2014), we investigated the potential immunomodulatory effect of LXA_4 pre-treatment on different T cell subsets from control or patients with relapsing-remitting MS. The observed LXA_4-induced reduction of the inflammatory profile in both activated cytotoxic human $CD8^+$ T cells as well as $CD4^+$ T cells is supported by recent findings showing that other SPMs, like RvD1, RvD2, and Mar1, modulate T cell responses (Chiurchiù et al., 2016), suggesting that these SPMs are also involved in the modulation of chronic inflammation (Serhan, 2014) via acting on cells of the adaptive arm of the immune system (Chiurchiù et al., 2016; Hsiao et al., 2015; Poisson et al., 2015; Schwanke et al., 2016). However, T cell subsets from patients with relapsing-remitting MS are less responsive to the immunomodulatory activity of LXA_4 compared to T cells from healthy controls. A possible explanation might be that these cells express reduced levels of its receptor ALX/FPR2 (Hodges et al., 2017; Maddox et al., 1997) or show an impaired intracellular signaling. For instance, it was recently reported that T cells of patients with chronic heart failure display reduced levels of another pro-resolving receptor, i.e., GPR32, making them less responsive and dysfunctional to the action of another SPM, i.e., RvD1 (Chiurchiù et al., 2019). Moreover, LXA_4 receptor (ALX/FPR2) is also expressed by other cell types involved in the neuro-inflammatory process, including macrophages, astrocytes, and microglia (Chiang and Serhan, 2017), and further research is warranted to define potential LXA_4-mediated effects on such cell types.

Besides T cell infiltrates, an EAE/MS lesion is also characterized by glial cell activation, resulting in a pro-inflammatory environment that causes neuronal tissue damage. We here characterized this inflammatory milieu in more detail by performing LC-MS/MS-based lipid mediator metabololipidomics together with authentic biologically derived and synthetic standards to establish a spinal cord lipid mediator signature profile under control and neuro-inflammatory conditions. We identified lipid mediators from each of the ω-6 AA, ω-3 DHA, and EPA bioactive metabolomes and revealed that CNS inflammation predominantly affected the AA bioactive metabolome, confirmed by significantly increased expression levels of pro-inflammatory lipid mediators, like PGE_2, PGD_2, PGF_{2a}, LTB_4, and TXB_2. These mediators are functionally characterized in inflammation and its resolution, and their biosynthetic pathways give rise to specific stereochemistry for each of these local mediators (Serhan and Petasis, 2011). Interestingly, we observed that LXA_4 treatment exclusively altered the expression levels of such pro-inflammatory lipid mediators during EAE, while leaving other SPMs unaffected. Principal-component analysis further revealed that the lipid mediator signature of various stages of EAE was normalized to a homeostatic signature upon LXA_4 treatment. Hence, bioactive lipid mediators are amenable to provide information regarding the potential inflammatory and/or resolution status of a given target tissue (for example, human lymph node tissues as described previously; Colas et al., 2014; Mangalam et al., 2013), which in turn can be used for both diagnosis in terms of biomarkers as well as personalized medicine (Norris and Serhan, 2018).

Our results, together with earlier findings (Chiurchiù et al., 2016; Geem et al., 2015; Luo et al., 2016; Ohse et al., 2004; Poisson et al., 2015; Schwab et al., 2007), suggest that LXA_4-mediated neuro-protection during EAE might be the result of different mechanisms, pointing toward a reduction in T cell CNS numbers by affecting their migration capacity as well as downregulation of pro-inflammatory capacities of the T cells. Additionally, we provide evidence that LXA_4 may also locally affect the lipidome of EAE spinal cord tissues, either directly or as a result of mechanisms mentioned above. Hence, further research is needed in order to better characterize molecular mechanisms associated with the protective effect of LXA_4 treatment during EAE. Finally, optimization of the injection route, doses, therapeutic approach, and mode of action are vital steps to be undertaken toward human clinical translation. Overall, our findings in the experimental

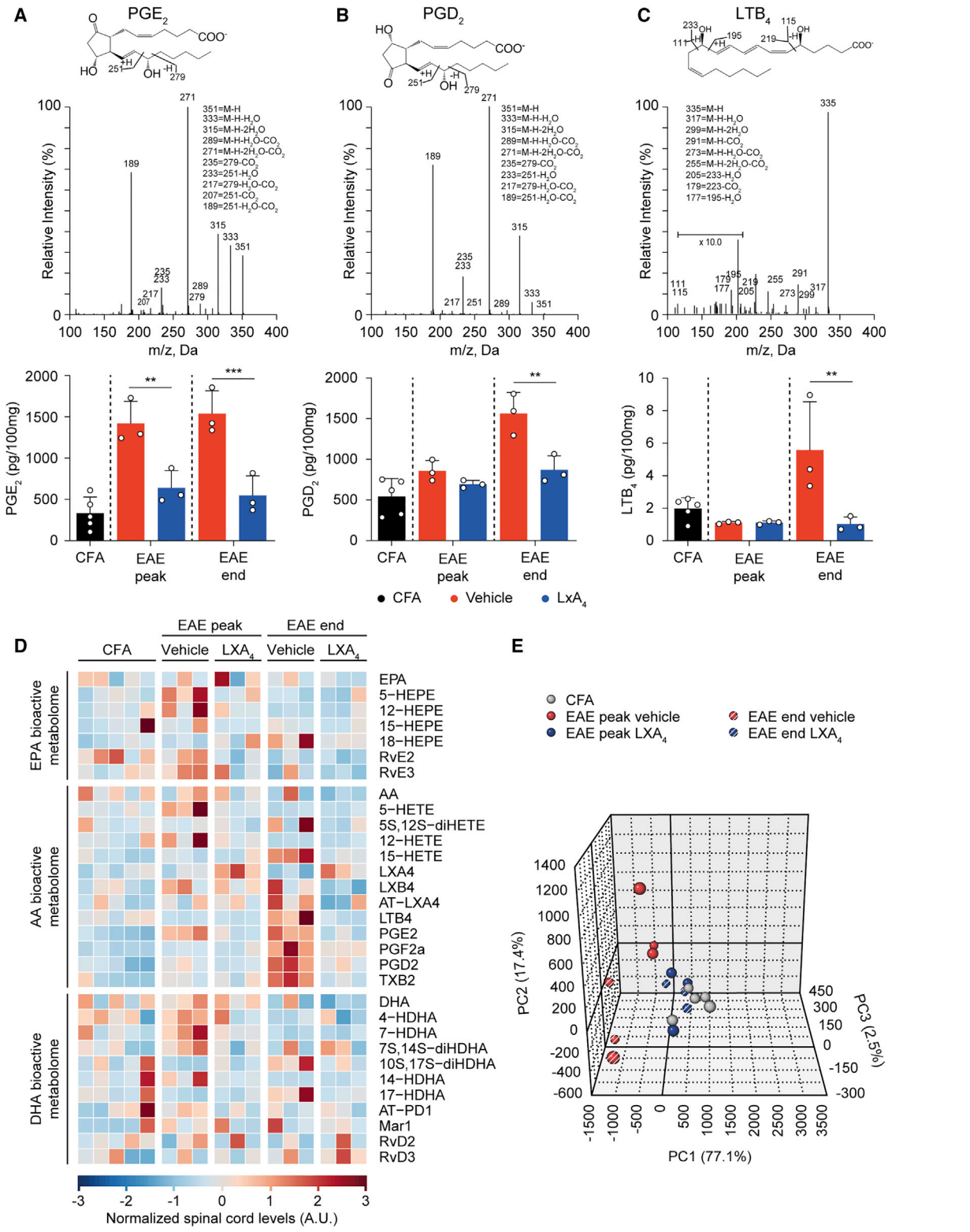

Figure 4. Normalization of EAE-induced spinal cord lipidome upon LXA_4 treatment

Lipid mediators were isolated from total spinal cords of control CFA (black bars) mice, EAE-vehicle (red bars)-treated mice, or LXA_4-treated (day 8–30 p.i.; blue bars), sacrificed at the peak of the disease (day 21 p.i.) and at the end of the disease (day 30 p.i.; CFA: n = 5 mice; all other groups: n = 3 mice), and individually analyzed by LC-MS/MS.

(legend continued on next page)

model of MS, supported also by the analogous data on patients with MS, suggest that LXA_4 treatment can be used to resolve neuro-inflammation and may represent an innovative and safe strategy to manage MS pathogenesis and potentially its progression.

STAR★METHODS

Detailed methods are provided in the online version of this paper and include the following:

- KEY RESOURCES TABLE
- RESOURCE AVAILABILITY
  - Lead contact
  - Materials availability
  - Data and code availability
- EXPERIMENTAL MODEL AND SUBJECT DETAILS
  - Mice and EAE induction
  - Human cells
- METHOD DETAILS
  - Human T-lymphocyte treatments
  - Immunohistochemistry
  - Spinal cord dissociation
  - Flow cytometry analysis
  - LC-MS/MS based lipid mediator metabololipidomics
  - Principal component analysis
  - Transwell migration of human $CD4^+$ and $CD8^+$ T cells
- QUANTIFICATION AND STATISTICAL ANALYSIS

SUPPLEMENTAL INFORMATION

Supplemental information can be found online at https://doi.org/10.1016/j.celrep.2021.109201.

ACKNOWLEDGMENTS

This work was supported by the European Union's Seventh Framework Program FP7 under grant agreement 607962 (nEUROinflammation), the Swiss Multiple Sclerosis Society (grant SMSS2016 to G.E. and G.K.), the Nauta Fonds and VUmc MS Center Amsterdam (G.K.), an IBRO Research Fellowship (G.K.), grants from the Dutch MS Research Foundation (grants 14-878MS and 18-1023 to G.K.), the Dutch Research Council (NWO Vidi grant 91719305 to G.K.), the Italian Foundation of Multiple Sclerosis (grant FISM 2017/R/08), and the Italian Ministry of Health grant (GR-2016-02362380 to V.C.). Studies in Boston were supported by NIH (grant 5P01GM095467-07) to C.N.S. We thank Dr. Urban Deutsch for help with the mouse housing and logistics. Additional thanks go to Katrin Bissegger, Isabelle Wymann, and Svetlozar Tsonev for professional caretaking of the mice and help with the experimental design.

AUTHOR CONTRIBUTIONS

G.K., B.E., H.E.d.V., and V.C. designed research studies; C.D.T., G.E., V.C., S.M.T., M.S., A.K., N.H.J., and S.M.A.v.d.P. conducted experiments; C.D.T., G.E., V.C., A.K., and G.K. analyzed the data; P.C.N. and G.K. conducted metabololipidomics analyses; A.L. helped in some experiments on T cells; G.K., V.C., B.E., H.E.d.V., and C.N.S. provided reagents; C.N.S., B.E., and H.E.d.V. provided scientific suggestions; G.K., C.D.T., and V.C. wrote the manuscript; and C.N.S., B.E., and H.E.d.V. revised the manuscript.

DECLARATION OF INTERESTS

The authors declare no competing interests.

Received: September 4, 2019
Revised: June 30, 2020
Accepted: May 11, 2021
Published: June 1, 2021

REFERENCES

Bisicchia, E., Sasso, V., Catanzaro, G., Leuti, A., Besharat, Z.M., Chiacchiarini, M., Molinari, M., Ferretti, E., Viscomi, M.T., and Chiurchiù, V. (2018). Resolvin D1 halts remote neuroinflammation and improves functional recovery after focal brain damage via ALX/FPR2 receptor-regulated microRNAs. Mol. Neurobiol. *55*, 6894–6905.

Bogie, J.F.J., Haidar, M., Kooij, G., and Hendriks, J.J.A. (2020). Fatty acid metabolism in the progression and resolution of CNS disorders. Adv. Drug Deliv. Rev. *159*, 198–213.

Bonnans, C., Vachier, I., Chavis, C., Godard, P., Bousquet, J., and Chanez, P. (2002). Lipoxins are potential endogenous antiinflammatory mediators in asthma. Am. J. Respir. Crit. Care Med. *165*, 1531–1535.

Calder, P.C. (2006). Polyunsaturated fatty acids and inflammation. Prostaglandins Leukot. Essent. Fatty Acids *75*, 197–202.

Chiang, N., and Serhan, C.N. (2017). Structural elucidation and physiologic functions of specialized pro-resolving mediators and their receptors. Mol. Aspects Med. *58*, 114–129.

Chiurchiù, V. (2014). Novel targets in multiple sclerosis: to oxidative stress and beyond. Curr. Top. Med. Chem. *14*, 2590–2599.

Chiurchiù, V., Leuti, A., Dalli, J., Jacobsson, A., Battistini, L., Maccarrone, M., and Serhan, C.N. (2016). Proresolving lipid mediators resolvin D1, resolvin D2, and maresin 1 are critical in modulating T cell responses. Sci. Transl. Med. *8*, 353ra111.

Chiurchiù, V., Leuti, A., and Maccarrone, M. (2018). Bioactive lipids and chronic inflammation: managing the fire within. Front. Immunol. *9*, 38.

Chiurchiù, V., Leuti, A., Saracini, S., Fontana, D., Finamore, P., Giua, R., Padovini, L., Incalzi, R.A., and Maccarrone, M. (2019). Resolution of inflammation is altered in chronic heart failure and entails a dysfunctional responsiveness of T lymphocytes. FASEB J. *33*, 909–916.

Colas, R.A., Shinohara, M., Dalli, J., Chiang, N., and Serhan, C.N. (2014). Identification and signature profiles for pro-resolving and inflammatory lipid mediators in human tissue. Am. J. Physiol. Cell Physiol. *307*, C39–C54.

Compston, A., and Coles, A. (2008). Multiple sclerosis. Lancet *372*, 1502–1517.

Cotsapas, C., and Mitrovic, M. (2018). Genome-wide association studies of multiple sclerosis. Clin. Transl. Immunology *7*, e1018.

Dalli, J., and Serhan, C.N. (2012). Specific lipid mediator signatures of human phagocytes: microparticles stimulate macrophage efferocytosis and pro-resolving mediators. Blood *120*, e60–e72.

Engelhardt, B., and Ransohoff, R.M. (2005). The ins and outs of T-lymphocyte trafficking to the CNS: anatomical sites and molecular mechanisms. Trends Immunol. *26*, 485–495.

(A–C) Representative MS/MS spectra of PGE_2 (A), PGD_2 (B), and LTB_4 (C) and data are presented as mean (pg/100 mg spinal cord) ± SEM. $^{**}p < 0.01$ and $^{***}p < 0.001$ determined by one-way ANOVA followed by post hoc Bonferroni correction.
(D) Heatmap of lipid mediator profiles under control or during different EAE phases upon LXA_4/vehicle treatment. Columns represent different experimental groups and individual mice. The relative value for each lipid mediator is depicted by color intensity, with blue indicating decreased and red indicating increased lipid mediator levels.
(E) Unbiased principal-component analysis reveals temporal clustering of identified lipid mediator signatures in each experimental condition.

Geem, D., Harusato, A., Flannigan, K., and Denning, T.L. (2015). Harnessing regulatory T cells for the treatment of inflammatory bowel disease. Inflamm. Bowel Dis. *21*, 1409–1418.

Gentile, A., De Vito, F., Fresegna, D., Rizzo, F.R., Bullitta, S., Guadalupi, L., Vanni, V., Buttari, F., Stampanoni Bassi, M., Leuti, A., et al. (2020). Peripheral T cells from multiple sclerosis patients trigger synaptotoxic alterations in central neurons. Neuropathol. Appl. Neurobiol. *46*, 160–170.

Gilroy, D.W., Lawrence, T., Perretti, M., and Rossi, A.G. (2004). Inflammatory resolution: new opportunities for drug discovery. Nat. Rev. Drug Discov. *3*, 401–416.

Han, S., Lin, Y.C., Wu, T., Salgado, A.D., Mexhitaj, I., Wuest, S.C., Romm, E., Ohayon, J., Goldbach-Mansky, R., Vanderver, A., et al. (2014). Comprehensive immunophenotyping of cerebrospinal fluid cells in patients with neuroimmunological diseases. J. Immunol. *192*, 2551–2563.

Hawkins, K.E., DeMars, K.M., Singh, J., Yang, C., Cho, H.S., Frankowski, J.C., Doré, S., and Candelario-Jalil, E. (2014). Neurovascular protection by post-ischemic intravenous injections of the lipoxin A4 receptor agonist, BML-111, in a rat model of ischemic stroke. J. Neurochem. *129*, 130–142.

Hawkins, K.E., DeMars, K.M., Alexander, J.C., de Leon, L.G., Pacheco, S.C., Graves, C., Yang, C., McCrea, A.O., Frankowski, J.C., Garrett, T.J., et al. (2017). Targeting resolution of neuroinflammation after ischemic stroke with a lipoxin A_4 analog: protective mechanisms and long-term effects on neurological recovery. Brain Behav. *7*, e00688.

Hellberg, S., Eklund, D., Gawel, D.R., Köpsén, M., Zhang, H., Nestor, C.E., Kockum, I., Olsson, T., Skogh, T., Kastbom, A., et al. (2016). Dynamic response genes in CD4+ T cells reveal a network of interactive proteins that classifies disease activity in multiple sclerosis. Cell Rep. *16*, 2928–2939.

Hodges, R.R., Li, D., Shatos, M.A., Bair, J.A., Lippestad, M., Serhan, C.N., and Dartt, D.A. (2017). Lipoxin A_4 activates ALX/FPR2 receptor to regulate conjunctival goblet cell secretion. Mucosal Immunol. *10*, 46–57.

Hsiao, H.-M., Thatcher, T.H., Colas, R.A., Serhan, C.N., Phipps, R.P., and Sime, P.J. (2015). Resolvin D1 reduces emphysema and chronic inflammation. Am. J. Pathol. *185*, 3189–3201.

Kong, W., Yen, J.-H., and Ganea, D. (2011). Docosahexaenoic acid prevents dendritic cell maturation, inhibits antigen-specific Th1/Th17 differentiation and suppresses experimental autoimmune encephalomyelitis. Brain Behav. Immun. *25*, 872–882.

Kooij, G., van Horssen, J., de Lange, E.C., Reijerkerk, A., van der Pol, S.M., van Het Hof, B., Drexhage, J., Vennegoor, A., Killestein, J., Scheffer, G., et al. (2010). T lymphocytes impair P-glycoprotein function during neuroinflammation. J. Autoimmun. *34*, 416–425.

Kooij, G., Mizee, M.R., van Horssen, J., Reijerkerk, A., Witte, M.E., Drexhage, J.A., van der Pol, S.M., van het Hof, B., Scheffer, G., and Scheper, R. (2011). Adenosine triphosphate-binding cassette transporters mediate chemokine (C-C motif) ligand 2 secretion from reactive astrocytes: relevance to multiple sclerosis pathogenesis. Brain *134*, 555–570.

Kooij, G., Kroon, J., Paul, D., Reijerkerk, A., Geerts, D., van der Pol, S.M., van Het Hof, B., Drexhage, J.A., van Vliet, S.J., Hekking, L.H., et al. (2014). P-glycoprotein regulates trafficking of CD8(+) T cells to the brain parenchyma. Acta Neuropathol. *127*, 699–711.

Kooij, G., Troletti, C.D., Leuti, A., Norris, P.C., Riley, I., Albanese, M., Ruggieri, S., Libreros, S., van der Pol, S.M.A., van Het Hof, B., et al. (2020). Specialized pro-resolving lipid mediators are differentially altered in peripheral blood of patients with multiple sclerosis and attenuate monocyte and blood-brain barrier dysfunction. Haematologica *105*, 2056–2070.

Krashia, P., Cordella, A., Nobili, A., La Barbera, L., Federici, M., Leuti, A., Campanelli, F., Natale, G., Marino, G., Calabrese, V., et al. (2019). Blunting neuroinflammation with resolvin D1 prevents early pathology in a rat model of Parkinson's disease. Nat. Commun. *10*, 3945.

Lassmann, H. (2005). Multiple sclerosis pathology: evolution of pathogenetic concepts. Brain Pathol. *15*, 217–222.

Lassmann, H. (2014). Mechanisms of white matter damage in multiple sclerosis. Glia *62*, 1816–1830.

Leuti, A., Maccarrone, M., and Chiurchiù, V. (2019). Proresolving lipid mediators: endogenous modulators of oxidative stress. Oxid. Med. Cell. Longev. *2019*, 8107265.

Luo, C.-L., Li, Q.-Q., Chen, X.-P., Zhang, X.-M., Li, L.-L., Li, B.-X., Zhao, Z.-Q., and Tao, L.-Y. (2013). Lipoxin A4 attenuates brain damage and downregulates the production of pro-inflammatory cytokines and phosphorylated mitogen-activated protein kinases in a mouse model of traumatic brain injury. Brain Res. *1502*, 1–10.

Luo, B., Han, F., Xu, K., Wang, J., Liu, Z., Shen, Z., Li, J., Liu, Y., Jiang, M., Zhang, Z.-Y., and Zhang, Z. (2016). Resolvin D1 programs inflammation resolution by increasing TGF-β expression induced by dying cell clearance in experimental autoimmune neuritis. J. Neurosci. *36*, 9590–9603.

Maddox, J.F., Hachicha, M., Takano, T., Petasis, N.A., Fokin, V.V., and Serhan, C.N. (1997). Lipoxin A4 stable analogs are potent mimetics that stimulate human monocytes and THP-1 cells via a G-protein-linked lipoxin A4 receptor. J. Biol. Chem. *272*, 6972–6978.

Mangalam, A., Poisson, L., Nemutlu, E., Datta, I., Denic, A., Dzeja, P., Rodriguez, M., Rattan, R., and Giri, S. (2013). Profile of circulatory metabolites in a relapsing-remitting animal model of multiple sclerosis using global metabolomics. J. Clin. Cell. Immunol. *4*. https://doi.org/10.4172/2155-9899.1000150.

Martini, A.C., Berta, T., Forner, S., Chen, G., Bento, A.F., Ji, R.-R., and Rae, G.A. (2016). Lipoxin A4 inhibits microglial activation and reduces neuroinflammation and neuropathic pain after spinal cord hemisection. J. Neuroinflammation *13*, 75.

Medeiros, R., Kitazawa, M., Passos, G.F., Baglietto-Vargas, D., Cheng, D., Cribbs, D.H., and LaFerla, F.M. (2013). Aspirin-triggered lipoxin A4 stimulates alternative activation of microglia and reduces Alzheimer disease-like pathology in mice. Am. J. Pathol. *182*, 1780–1789.

Newson, J., Stables, M., Karra, E., Arce-Vargas, F., Quezada, S., Motwani, M., Mack, M., Yona, S., Audzevich, T., and Gilroy, D.W. (2014). Resolution of acute inflammation bridges the gap between innate and adaptive immunity. Blood *124*, 1748–1764.

Norris, P.C., and Serhan, C.N. (2018). Metabololipidomic profiling of functional immunoresolvent clusters and eicosanoids in mammalian tissues. Biochem. Biophys. Res. Commun. *504*, 553–561.

Ohse, T., Ota, T., Kieran, N., Godson, C., Yamada, K., Tanaka, T., Fujita, T., and Nangaku, M. (2004). Modulation of interferon-induced genes by lipoxin analogue in anti-glomerular basement membrane nephritis. J. Am. Soc. Nephrol. *15*, 919–927.

Poisson, L.M., Suhail, H., Singh, J., Datta, I., Denic, A., Labuzek, K., Hoda, M.N., Shankar, A., Kumar, A., Cerghet, M., et al. (2015). Untargeted plasma metabolomics identifies endogenous metabolite with drug-like properties in chronic animal model of multiple sclerosis. J. Biol. Chem. *290*, 30697–30712.

Prüss, H., Rosche, B., Sullivan, A.B., Brommer, B., Wengert, O., Gronert, K., and Schwab, J.M. (2013). Proresolution lipid mediators in multiple sclerosis - differential, disease severity-dependent synthesis - a clinical pilot trial. PLoS ONE *8*, e55859.

Reich, D.S., Lucchinetti, C.F., and Calabresi, P.A. (2018). Multiple sclerosis. N. Engl. J. Med. *378*, 169–180.

Ren, H., Yang, Z., Luo, C., Zeng, H., Li, P., Kang, J.X., Wan, J.-B., He, C., and Su, H. (2017). Enriched endogenous omega-3 fatty acids in mice ameliorate parenchymal cell death after traumatic brain injury. Mol. Neurobiol. *54*, 3317–3326.

Sawcer, S., Hellenthal, G., Pirinen, M., Spencer, C.C., Patsopoulos, N.A., Moutsianas, L., Dilthey, A., Su, Z., Freeman, C., Hunt, S.E., et al.; International Multiple Sclerosis Genetics Consortium; Wellcome Trust Case Control Consortium 2 (2011). Genetic risk and a primary role for cell-mediated immune mechanisms in multiple sclerosis. Nature *476*, 214–219.

Schwab, J.M., Chiang, N., Arita, M., and Serhan, C.N. (2007). Resolvin E1 and protectin D1 activate inflammation-resolution programmes. Nature *447*, 869–874.

Schwanke, R.C., Marcon, R., Bento, A.F., and Calixto, J.B. (2016). EPA- and DHA-derived resolvins' actions in inflammatory bowel disease. Eur. J. Pharmacol. *785*, 156–164.

Serhan, C.N. (2005). Lipoxins and aspirin-triggered 15-epi-lipoxins are the first lipid mediators of endogenous anti-inflammation and resolution. Prostaglandins Leukot. Essent. Fatty Acids *73*, 141–162.

Serhan, C.N. (2014). Pro-resolving lipid mediators are leads for resolution physiology. Nature *510*, 92–101.

Serhan, C.N., and Petasis, N.A. (2011). Resolvins and protectins in inflammation resolution. Chem. Rev. *111*, 5922–5943.

Stys, P.K., Zamponi, G.W., van Minnen, J., and Geurts, J.J. (2012). Will the real multiple sclerosis please stand up? Nat. Rev. Neurosci. *13*, 507–514.

Tabas, I., and Glass, C.K. (2013). Anti-inflammatory therapy in chronic disease: challenges and opportunities. Science *339*, 166–172.

Tietz, S.M., Zwahlen, M., Haghayegh Jahromi, N., Baden, P., Lazarevic, I., Enzmann, G., and Engelhardt, B. (2016). Refined clinical scoring in comparative EAE studies does not enhance the chance to observe statistically significant differences. Eur. J. Immunol. *46*, 2481–2483.

Wang, X., Zhu, M., Hjorth, E., Cortés-Toro, V., Eyjolfsdottir, H., Graff, C., Nennesmo, I., Palmblad, J., Eriksdotter, M., Sambamurti, K., et al. (2015). Resolution of inflammation is altered in Alzheimer's disease. Alzheimers Dement. *11*, 40–50.e2.

Weksler, B.B., Subileau, E.A., Perrière, N., Charneau, P., Holloway, K., Leveque, M., Tricoire-Leignel, H., Nicotra, A., Bourdoulous, S., Turowski, P., et al. (2005). Blood-brain barrier-specific properties of a human adult brain endothelial cell line. FASEB J. *19*, 1872–1874.

Wu, Y., Ye, X.-H., Guo, P.-P., Xu, S.-P., Wang, J., Yuan, S.-Y., Yao, S.-L., and Shang, Y. (2010). Neuroprotective effect of lipoxin A4 methyl ester in a rat model of permanent focal cerebral ischemia. J. Mol. Neurosci. *42*, 226–234.

Wu, L., Liu, Z.J., Miao, S., Zou, L.B., Cai, L., Wu, P., Ye, Y., Wu, Q., and Li, H.H. (2013). Lipoxin A4 ameliorates cerebral ischaemia/reperfusion injury through upregulation of nuclear factor erythroid 2-related factor 2. Neurol. Res. *35*, 968–975.

Ye, X.-H., Wu, Y., Guo, P.-P., Wang, J., Yuan, S.-Y., Shang, Y., and Yao, S.-L. (2010). Lipoxin A4 analogue protects brain and reduces inflammation in a rat model of focal cerebral ischemia reperfusion. Brain Res. *1323*, 174–183.

STAR★METHODS

KEY RESOURCES TABLE

REAGENT or RESOURCE	SOURCE	IDENTIFIER
Antibodies		
rabbit-anti-CD4	Abcam	Cat# ab183685; RRID: AB_2686917
rat-anti-CD45	BDBioscience	Cat# 553076; RRID: AB_394606
rabbit-anti-CD8	Abcam	Cat# ab217344; RRID: B_2890649
rabbit-anti-collagen IV	Abcam	RRID: AB_305584
donkey-anti-rabbit Alexa488	Molecular Probes	Cat# A21206; RRID: AB_2535792
goat-anti-rat Alexa555	Molecular Probes	Cat# A21434; RRID: AB_141733
Streptavidin Alexa647	Molecular Probes	Cat# S32357; RRID: AB_2336066
anti-mouse CD4 PerCP5.5	Biolegend	Cat# RM4-5; RRID: AB_893325
anti-mouse CD8 FITC	Biolegend	Cat# 5H10-1; RRID: AB_312764
anti-mouse TNF-α PE-Cy7	Biolegend	Cat# MP6-XT22; RRID: AB_2204356
anti-mouse IFN-γ APC	Biolegend	Cat# XMG1.2; RRID: AB_315404
anti-mouse IL-17 PE	Biolegend	Cat# TC11-18H10.1; RRID: AB_315464
anti-mouse CD4 APC/Fire-750	Biolegend	Cat# RM4-5; RRID: AB_2629699
anti-mouse CD8 PerCP-eFluor 710	BD Biosciences	Cat# 53-6.7; RRID: AB_1603266
anti-mouse CD45 PE-Cy7	LSBio	Cat# LS-C810960
anti-mouse CD11b FITC	BD Biosciences	Cat# M1/70; RRID: AB_394774
anti-mouse Ly6c FITC	Biolegend	Cat# HK1.4; RRID: AB_1186134
anti-mouse TNF-α BV650	BD Biosciences	Cat# MP6-XT22; RRID: AB_2738498
anti-mouse IFN-γ APC	Biolegend	Cat# XMG1.2; RRID: AB_315404
anti-mouse IL-17 PE	Biolegend	Cat# TC11-18H10.1; RRID: AB_315464
anti-human CD4 e780	BD Biosciences	Cat# RPA-T4; RRID: AB_1272044
anti-human CD8 Brilliant Violet 421	Biolegend	Cat# SK1; RRID: AB_2629583
anti-human CD25 ECD	Beckman Coulter	Cat# 6607112
anti-human TNF-α PE-Cy7	BD Biosciences	Cat# Mab11; RRID: AB_1727578
anti-human IFN-γ APC	BD Biosciences	Cat# 4S.B3; RRID: AB_398505
anti-human IL-17 PE	BD Biosciences	Cat# 033-782; RRID: AB_1645512
Biological samples		
Human PBMC	Santa Lucia Foundation Biobank (Rome, Italy)	N/A
Chemicals, peptides, and recombinant proteins		
Lipoxin A_4 (LXA_4)	Cayman Chemical	Cat# 90410
Lipoxin A_4 methyl ester (LXA_4-ME)	Cayman Chemical	Cat# 10033
Myelin oligodendrocyte glycoprotein aa35-55	GenScript	Cat# RP10245
Incomplete Freund's adjuvant	Santa Cruz	Cat# sc-24648; RRID: AB_10186533
Mycobacterium tuberculosis	BD Biosciences	Cat# 231141
Pertussis toxin	List Biologica Laboratories	Cat# 180
Saline	Braun	Cat# 2132363
Isoflurane	Piramal Healthcare	Cat# NDC 66794-017-25
Paraformaldehyde	Merck	Cat# 1.04005.1000
DPBS	GIBCO	Cat# 14190-094
Ficoll-Paque PLUS	GE Healthcare	Cat# 17-1440-02
Brefeldin-A	Sigma Aldrich	Cat# B7651

(*Continued on next page*)

Continued

REAGENT or RESOURCE	SOURCE	IDENTIFIER
Tissue-Tek OCT compound	Sakura Europe	Cat# 25608-930
2-methylbutane	Sigma-Aldrich	Cat# 78-78-4
Triton X-100	Sigma-Aldrich	Cat# 9002-93-1
Normal goat serum	MP biomedicals	Cat# 8642921; RRID: AB_2335031
DAPI	Invitrogen	Cat# D1306; RRID: AB_2629482
Mowiol	Sigma-Aldrich	Cat# 81381
Sudan black	Sigma-Aldrich	Cat# 4197-25-5
collagenase type VIII	Sigma-Aldrich	Cat# C2139
DNase I	Sigma-Aldrich	Cat# 11284932001
Percoll	GE Healthcare	Cat# 17-0891-01
Zombie Near-IR Fixable viability dye	Biolegend	Cat# 423106
eFluor 506 Fixable viability dye	eBioscience	Cat# 65-0866-14
Cytofix/cytoperm	BD Biosciences	Cat# 554715; RRID: AB_2869008
Saponin	Sigma-Aldrich	Cat# 8047-15-2
Methanol	Sigma Aldrich	Cat# 32213
d8-5S-HETE	Cayman Chemical	Cat# 334230
d4-LTB_4	Cayman Chemical	Cat# 320110
d5-LXA_4	Cayman Chemical	Cat# 10007737
d4-PGE_2	Cayman Chemical	Cat# 314010
d5-RvD2	Cayman Chemical	Cat# 11184
C18 columns	Thermo Fisher	Cat# SI928975-906
Methyl formate	Sigma Aldrich	Cat# 291056
Collagen type 1	Sigma-Aldrich	Cat# C9791
Serum free medium	Invitrogen	Cat# A3705001
Beads / flow count fluorospheres	Beckman Coulter	Cat# 7547053
Critical commercial assays		
Dynabeads Human T-activator CD3/CD28 for T cell expansion and activation	ThermoFisher	Cat# 11161D
Experimental models: organisms/strains		
C57BL/6J female mice	Janvier (France)	N/A
Software and algorithms		
Graphpad Prism	https://www.graphpad.com	Version 7
FlowJo software	https://www.flowjo.com	v.10 (TreeStar)
SIMCA software	MKS Data Analytics Solution Umea	13.0.3
Imaris x64 software	Bitplane AG	version 9.1.2

RESOURCE AVAILABILITY

Lead contact

Further information and requests for resources and reagents should be directed to and will be fulfilled by the Lead Contact Gijs Kooij (g.kooij@amsterdamumc.nl).

Materials availability

This study did not generate new unique reagents.

Data and code availability

The published article includes all datasets generated or analyzed during this study

EXPERIMENTAL MODEL AND SUBJECT DETAILS

Mice and EAE induction

All applicable international, national, and institutional guidelines for the care and use of animals were followed. In detail, *in vivo* experiments were performed in accordance with the Swiss legislation on the protection of animals and were approved by the Veterinary Office of the Canton of Bern (licenses BE 42/14 and BE 28/16). Animal research was performed in accordance to the Swiss legislation on the protection of animals and in compliance with the ARRIVE guidelines for reporting animal research (https://arriveguidelines.org). To investigate the effect of LXA_4 treatment on EAE, we used a chemically stable variant called LXA_4-methyl ester (LXA_4-ME) and disease was induced in eight weeks old C57BL/6J female mice. Animals were purchased from Janvier (France), randomly assigned to different experimental groups of 10 mice and housed in individually ventilated cages (Table S1). Besides water and breeding chow *ad libitum*, the mice received tissues and paper rolls as animation tools. C57BL/6J female mice were immunized subcutaneously into both flanks and tail root with 200 μg of myelin oligodendrocyte glycoprotein aa35-55 (MOG_{33-55}) emulsified in 100 μL complete Freund's adjuvant (CFA) supplemented with Mycobacterium tuberculosis. At day zero and day two after immunization, 300 ng of pertussis toxin was applied intraperitoneal (i.p.). A control group was included that received only CFA and pertussis toxin. To study the prophylactic effect of LXA_4, EAE mice were injected daily from day eight of EAE with LXA_4 i.p. (100 ng/animal in a volume of 0.1 mL of 0.9% saline) until the end of the experiment (day 30). Animal welfare was assessed twice-daily; weight and disease progression was documented once daily and scored as follows: 0.5 (limp tail), 1 (hind leg weakness), 2 (hind leg paraparesis), 3 (hind leg paraparesis and incontinence) (Tietz et al., 2016). Wet chow was provided in a Petri dish and renewed daily as soon as the first mouse reached a clinical score of 1. To investigate whether LXA_4 withdrawal causes a rebound effect, weight and clinical scores were continuously assessed until the end of the experiment. At the peak and the end of the experiment, i.e., at day 21 and 30 p.i., mice were deeply anesthetized with isoflurane and perfused transcardial with 1% paraformaldehyde in PBS, pH 7.4. Afterward, brain and spinal cord were collected and processed for immunohistological analysis. For LC-MS/MS and flow cytometry analysis, anesthetized mice were perfused transcardial with PBS, pH 7.4 only.

Human cells

Peripheral blood mononuclear cells (PBMC) from healthy controls (n = 6, all women, mean 33.8 ± 3.7 years) and patients with RR-MS (n = 6, all women, mean age 33.7 ± 6.5 years, see Table S4 for demographics) were separated by density gradient using Ficoll, according to standard procedures. The diagnosis of MS was established at the end of the diagnostic protocol by clinical, laboratory, and magnetic resonance imaging parameters, and matched published criteria. The Expanded Disability Status Scale scores were always < 3 for patients with relapsing-remitting MS and all were treatment-naive at the time of sampling. Healthy control subjects had no history of autoimmune or degenerative diseases of the central or peripheral nervous system. All the subjects gave their written informed consent to the study. The ethics committees of Tor Vergata Hospital and of San Camillo Hospital approved the study.

METHOD DETAILS

Human T-lymphocyte treatments

PBMC from healthy subjects or patients with MS were left untreated or were pretreated with LXA_4 (10 nM, the most efficient working dose on immune cells, as reported (Bonnans et al., 2002; Chiurchiù et al., 2016) and then stimulated with Dynabeads CD3/CD28 T Cell Expander (one bead per cell) for eight hours to allow cytokine synthesis and in presence of 10 μg/ml brefeldin-A to inhibit cytokine secretion. Cells were subsequently analyzed by flow cytometry analysis (see below).

Immunohistochemistry

For immunohistochemistry, collected spinal cord was embedded in Tissue-Tek, and frozen in a dry ice-cooled 2-methylbutane bath. Immunofluorescence stainings were performed on 6-μm cryostat sections (n = 3 mice/group) as follows: after fixation in ice-cold acetone, sections were permeabilized with 0.1% Triton X-100, incubated for 30 min with 10% donkey serum and incubated overnight at 4°C with primary antibody against CD45, CD4 and CD8. The primary antibodies were visualized by incubation with donkey anti-rabbit Alexa488 and goat anti-rat Alexa555 for 1h at room temperature (RT). Next, to visualize endothelial cells, sections were first incubated for 30 min with 10% rabbit serum followed by incubation with a biotin-conjugated Collagen IV primary antibody overnight at 4°C. Collagen IV was visualized by incubation with streptavidin Alexa647 for 1h at RT. Sections were treated with Sudan Black (0.3% Sudan Black in 70% ethanol). DAPI was used for nuclear staining and slides were mounted in Mowiol. Slides were scanned on the Vectra Polaris whole-slide scanner (PerkinElmer, USA) at 20x magnification. NIS elements general analysis 3 (Version 5.30.00, Nikon Instruments Inc., USA) was used to automatically quantify the number of all $CD45^+$, $CD45^+CD4^+$ and $CD45^+CD8^+$ cells both in the whole tissue as well as in the vasculature (marked by Collagen IV). The final density of infiltrating cells was calculated by dividing the number of cells over the total area of the imaged section.

Spinal cord dissociation

At peak of EAE, eight animals per group were anesthetized and transcardially perfused with 10 mL of cold phosphate buffered saline (PBS) pH 7.4. Spinal cords were dissected, minced, and individually processed by enzymatic digestion in 1 mg/ml Collagenase and

1 μl/ml DNase in Hank's Balanced Salt Solution (HBSS) at 37°C for 30 min. Using a glass potter, pellets were manually homogenized in dissection medium containing 50 mL HBSS, 750 μL HEPES buffer and 650 μL glucose (45%). Infiltrated cells were isolated by 37% Percoll density gradient centrifugation. Lastly, the cells were passed through a 70 μm cell strainer and kept on ice until further analysis.

Flow cytometry analysis

For the flow cytometry analysis of infiltrated T cells in the spinal cord, cells were stained for surface antigens with PE-Cy7-conjugated anti-CD45 (1:80), PerCP-eFluor710-conjugated anti-CD8 (1:100), APC/Fire750-conjugated anti-CD4 (1:100), FITC-conjugated anti-CD11b and anti-Ly6c (1:100), made permeable with BD Cytofix/Cytoperm (Fixation/Permeabilization Solution Kit), and then stained intracellular with BV650-conjugated anti-TNF-α (1:80), APC-conjugated anti-IFN-γ (1:80), PE-conjugated anti–IL-17 (1:40) in BD Perm/Wash buffer at 4°C for 30 min. Dead cells were stained with the fixable viability dye eFluor 506. Spinal cord cells were analyzed by Attune NxT flow cytometer (ThermoFisher) and analyzed using FlowJo software. For mouse T cell flow cytometry analysis, total PBMC were stained for surface antigens with PerCP5.5-conjugated anti-CD4 (1:100), FITC-conjugated anti-CD8 (1:100), made permeable with Cytofix/Cytoperm reagents, and then stained intracellular with PE-Cy7-conjugated anti-TNF-α (1:100), APC-conjugated anti-IFN-γ (1:100), PE-conjugated anti–IL-17 (1:30) in 0.5% saponin at room temperature for 30 min. For human T cell flow cytometry analysis, total PBMCs were stained for surface antigens with APC-e780-conjugated anti-CD14 (1:100), FITC-conjugated anti-CD3 (1:100), e780-conjugated anti-CD4 (1:100), Brilliant Violet-conjugated anti-CD8 (1:150) and ECD-conjugated anti-CD25 (1:40), made permeable with Cytofix/Cytoperm reagents (BD Biosciences), and then stained intracellular with PE-Cy7-conjugated anti-TNF-α (1:100, eBioscience), APC-conjugated anti-IFN-γ (1:100, eBioscience), PE-conjugated anti–IL-17 (1:30, PharMingen) in 0.5% saponin at room temperature for 30 min. The use of these markers allowed us to exclude $CD14^+$ monocytes and gate on lymphoid cells based on CD3 expression and subsequently gating on both $CD8^+$ and $CD4^+$ T cells in order to evaluate the intracellular production of their respective cytokines. The expression of the activation marker CD25 was evaluated on total $CD3^+$ T cells. Mouse and human peripheral blood cells were analyzed by Cytoflex flow cytometer (Beckman Coulter) and analyzed using FlowJo software.

LC-MS/MS based lipid mediator metabololipidomics

For LC-MS/MS analysis, 2ml ice-cold methanol was added to each spinal cord and the samples were profiled using metabololipidomics as described previously (Colas et al., 2014). In short, for lipid mediator profiling deuterated internal standards d8-5S-HETE, d4-LTB_4, d5-LXA_4, d4-PGE_2 and d5-RvD2 (500 pg each) representing each chromatographic region of identified lipid mediators were added to samples to perform quantification and assessment of sample recovery. Proteins were allowed to precipitate at −20°C overnight prior to centrifugation (1200 g at 4°C for 10 min) and then supernatants were taken to solid-phase extraction on C18 columns. Products were eluted using methyl formate, brought to dryness under nitrogen and suspended in methanol-water (50:50) for lipid mediators (Colas et al., 2014). The system consisted of a Qtrap 6500 (AB Sciex, Framingham, MA, USA) equipped with a Shimadzu SIL-20AC autoinjector, LC-20AD binary pump (Shimadzu, Kyoto, Japan), and an Agilent Eclipse Plus C18 column (100 mm x 4.6 mm x 1,8 μm). To identify and quantify lipid mediators, multiple reaction monitoring (MRM) was used with signature ion pairs Q1 (parent ion) to Q3 (characteristic daughter ion) for each molecule (Table 1). Identification was conducted by using published criteria with six diagnostic ions and retention time matching of standards (Colas et al., 2014).

Principal component analysis

Principal component analysis was performed using SIMCA 13.0.3 software following mean centering and unit variance scaling of lipid mediator amounts. Principal component analysis serves as an unbiased, multivariate projection designed to identify the systematic variation in a data matrix (the overall bioactive lipid mediator profile of each experimental condition) with lower dimensional plane using score plots and loading plots. The score plot shows the systematic clusters among the observations (closer plots presenting higher similarity in the data matrix). Loading plots describe the magnitude and the manner (positive or negative correlation) in which the measured lipid mediators/SPM contribute to the cluster separation in the score plot.

Transwell migration of human $CD4^+$ and $CD8^+$ T cells

The *in vitro* $CD4^+$ and $CD8^+$ T cell transendothelial cell migration assay was performed using a Transwell system (Costar, the Netherlands) with polycarbonate filters pore size of 5 μm, which were coated with collagen type 1 (Sigma-Aldrich, the Netherlands). Human brain endothelial cells (hCMEC/D3 cells) (Weksler et al., 2005) were cultured until confluence and subsequently stimulated with TNF-α (5ng/ml) for 24 hours in serum free medium. Human $CD4^+$ or $CD8^+$ T cells were isolated from buffy coat as previously described (Kooij et al., 2010, 2014) and resuspended in serum free medium in the presence of LXA_4 (10 nM) for 30 minutes. Ethanol-vehicle treated $CD4^+$ or $CD8^+$ T cells were used as control. Subsequently, $CD4^+$ or $CD8^+$ T cells were added to the transwell filters ($1x10^5$ cells/well) and incubated for 4 hours at 37°C and in 5% CO_2. To determine the number of migrated cells, transmigrated cells were transferred to FACS tubes, and 20.000 beads (Beckman Coulter, USA) were added to each sample. Samples were analyzed using a FACS Calibur (Becton Dickinson, Belgium) and the number of migrated T cells was determined based on 5.000 gated beads. The absolute number of migrated T cells is presented compared to the total number of T cells added to the upper chamber as described (Kooij et al., 2011). All experiments were performed in triplicate with three different human donors.

QUANTIFICATION AND STATISTICAL ANALYSIS

Results are shown as mean values with standard error of the mean (SEM). Statistical analysis was performed using GraphPad Prism software (v7 GraphPad Software). Comparisons between 2 experimental groups were made by unpaired Student t test and between > 2 groups by one-way ANOVA followed by post hoc Bonferroni correction. Clinical EAE scores and clinical parameters were analyzed by non-parametric (Mann-Whitney). Differences were considered significant at $p < 0.05$. All statistical tests are described in the figure legends.